北海道大学工学部研究報告
第150号（平成2年）

Bulletin of the Faculty of Engineering,
Hokkaido University, No. 150 (1990)

Influence of Graphite Nodule Size on the Impact Properties of Spheroidal Graphite Cast Iron

Noboru SHIRAMINE* Kazumichi SHIMIZU**
Toshikatsu NARITA*** and Toru NOGUCHI*

(Received December 26, 1989)

Abstract

Charpy impact tests were performed on ferritic spheroidal graphite cast irons with three different graphite nodule diameters, and the influence of nodule size on the transition behavior was discussed. The experiments showed that the transition temperature varied 50 -100°C for 12-50 μm mean graphite nodule diameters while the static strength were almost the same. Fracture appearance and the load vs. time curves showed that the ductile to brittle transition occurs when a limited amount of ductile cracks caused cleavage cracks, and this takes place at higher temperatures in specimens with large graphite nodules. SEM fractography showed that the large graphite nodules make it easier for cleavage cracks to initiate due to the large inter-nodule distance, which makes the plane strain state easy to achieve. In the brittle region, graphite nodules act as barriers to the crack propagation, and the large number of small graphite nodules cause the higher impact values. In the ductile region, a large number of small graphite nodules causes low resistance to unstable crack propagation because of easy dimple nucleation, and result in lower impact values in V-notched specimens although the effect is not apparent in notchless specimens.

1. Introduction

Recently, large castings such as casks for radioactive waste products, and housings and beds for large industrial equipment, are produced with spheroidal graphite cast irons. These castings have heavy sections or large variations in wall thicknesses, and matrix structures and graphite nodule sizes may vary considerably depending on the position in the castings. They result in various mechanical properties. In estimating the mechanical properties for the design and use of such castings, it is necessary to consider the effect of variations of the microstructure in the castings.

The influence of graphite nodule size on mechanical properties has been studied by many investigators[1-6], and the differences in the impact energy and the ductile to brittle transition temperature have been reported to be influenced by the nodule size. To explain the effect of nodule size, the role of graphite nodules on hindering or arresting crack propagation[1-4],

* Department of Mechanical Engineering II
** Oita National College of Technology
*** Nippon Steel, Muroran Plant

supression of twinning[5], and cell boundary segregation[3] have been suggested.

In this report, ferritized spheroidal graphite cast irons with three different mean nodule diameters were studied by Charpy impact tests, and the difference in fracture behavior was discussed by the load deflextion curves and SEM fractography.

2. Experiment

2.1 Specimens

Specimens were spheroidal graphite irons cast into three different molds, 60 mm diameter 300 mm long in a sand mold, S1, 20 mm diameter 250 mm long in a sand mold, S2, and 30 mm diameter 250 mm long in a metal mold, M, as shown in Fig. 1. Two heat levels with high and low silicon contents, A and B, were used, giving six specimens, S1A, S1B, S2A, S2B, MA and MB. Specimens were ferritized by annealing as described in Fig. 1, and test pieces for Charpy impact tests and tensile tests were machined.

The chemical composition of the specimens are shown in Table 1, the tensile strength, graphite nodule diameters, and other structural parameters are shown in Table 2. The chemical compositions of A and B are similar except that the Si content is higher in specimen A.

Microstructure of A specimens is shown in Fig. 2. The structure of the B specimens is almost the same as A, and the mean graphite nodule diameters are also similar, about 50 μm in S1, 30 μm in S2, and 12 μm in M. The graphite area fraction is 13-14% in S1 and S2 and

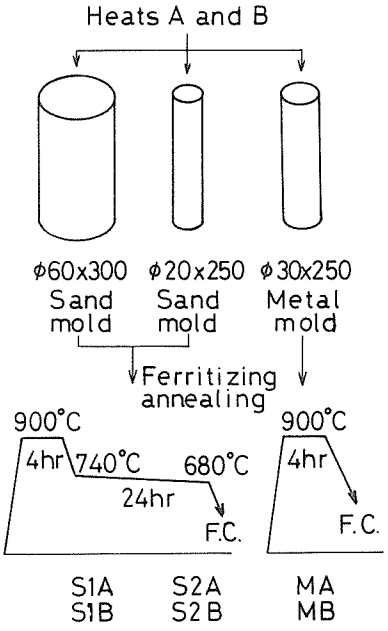

Fig. 1 Manufacture of the specimens

Table 1 Chemical composition of the specimens (wt. %)

		TC	GC	Si	Mn	P	S
A	S1A	3.84	3.59	2.73	0.49	0.026	0.016
	S2A	3.65	3.35				
	M A	3.71	3.54				
B	S1B	3.58	3.41	1.68	0.38	0.025	0.017
	S2B	3.92	3.60				
	M B	3.66	3.58				

Table 2 Tensile strength and structural parameters

		Tensile strength (Mpa)	Elongation (%)	Grahite area (%)	Mean nodule dia.(μm)	Ferrite grain size(μm)	Retained pearlite (%)
A	S1A	445	17	13	48	40	5
	S2A	430	17.5	13.5	34	28	3
	M A	450	18	11.5	12	22	>1
B	S1B	410	20	13	51	42	>1
	S2B	440	16	14	30	29	>1
	M B	450	18	11.5	12	21	2

11.5% in M, with nodularity about 90% in both specimens. These structural parameters were determined by a quantitative television microscope (image analyzer). The low graphite area fractions in MA and MB are inferred to be due to the measurement as the very small particles on the CRT image were neglected in the image analysis. The carbon analysis in MA and MB shows no indication of low graphite area fractions.

The average tensile strength of two test pieces of specimens S1A, S2A, and MA are similar despite the large differences in graphite nodule diameters and ferrite grain sizes, although smaller graphite diameters are reported to result in higher strengths and smaller elongations. High tensile strength in S1A may be caused by retained pearlite.

The S1B specimens show lower strengths than the other two B specimens.

2.2 Test pieces and instrumentation

Charpy impact tests were performed on standard notchless and V-notched specimens at 7 or 8 temperatures between 100 and −196°C depending on the specimens.

The impact tester was instrumented by strain gauges on the hammer and load vs. time curves were recorded on a digital transient memory scope. The absorbed energy calculated from the load time curve[7] agreed with the values from the Charpy indicator, within a 5% error for notchless specimens and more for V-notched specimens.

3. Results of experiment

3.1 Energy transition curves

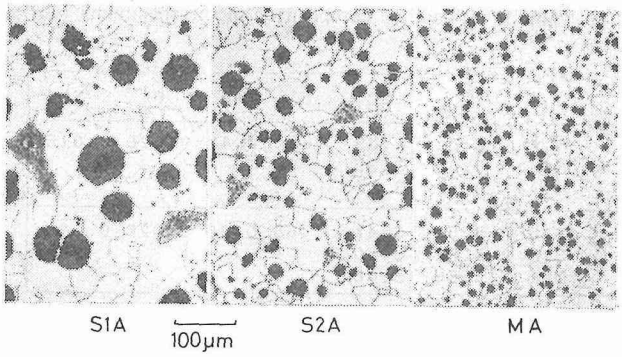

Fig. 2 Microstructure of the specimens (A specimens)

Table 3 Transition temperatures

		Notchless	V-notched
A	S1A	- 40	+ 30
	S2A	-110	- 30
	M A	-135	- 75
B	S1B	-110	- 35
	S2B	-140	- 75
	M B	-160	-100

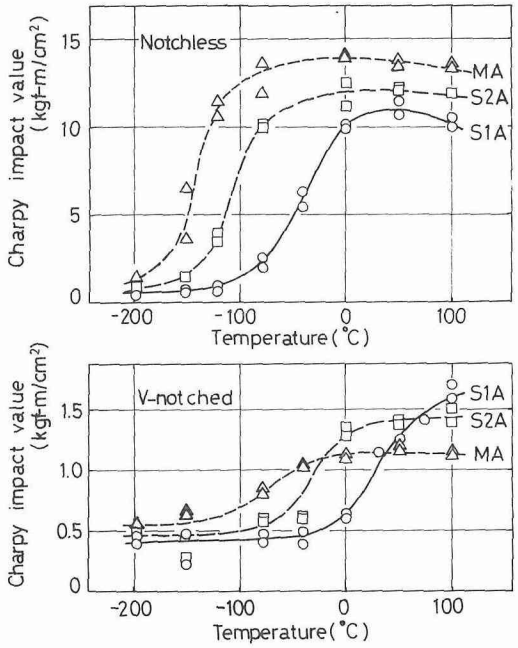

Fig. 3 Charpy energy transition curves of A specimens

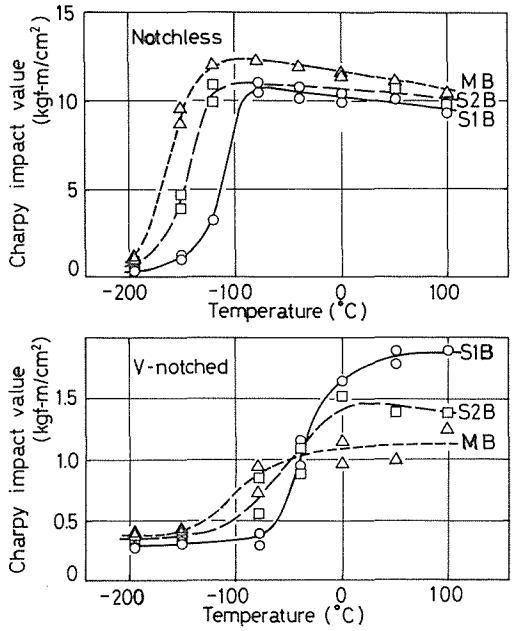

Fig. 4 Charpy energy transition curves of B specimens

Charpy energy transition curves for the notchless and V-notched A specimens are shown in Fig. 3, and B specimens in Fig. 4. In notchless specimens, smaller graphite nodules give higher impact values in the whole temperature region for both A and B[6]. Energy differences are small in the lower shelf region, larger in the upper shelf region, and is very large in the transition range resulting in large differences in transition temperatures. The higher impact values with larger graphite nodules reported by several investigators[3-5] were not observed in notchless specimens in the present experiments.

In V-notched specimens, however, larger graphite nodules show higher impact energy in the upper shelf region, and the curves cross in the transition range, and the order of impact values is in reverse of the lower shelf region both in A and B.

Energy transition temperatures defined by $\frac{1}{2}$ x (upper and lower shelf energy) are listed in Table. 3. The transition temperature in notchless S1A is −40°C, and −135°C in MA, a differece of more than 90°C. The transition temperature difference in V-notched specimens S1A and MA is more than 100°C. In the B specimens, transition terperatures are lower than in the A specimens, but the temperature differences are smaller, 50°C in notchless specimens, and 65°C in V-notched specimens.

In these specimens, ferrite grain size is not constant but varies as shown in Fig. 2 and Table 2, and may influence the transition temperature. According to the experiment by Shioda and Komatsu[4] using irons with 40 μm mean diameter graphite nodules, transition temperature differences due to 20 to 40 μm ferrite grain sizes are about 30°C. The temperature differences in the present experiments are larger than this, and this is inferred to be due to the graphite nodule size.

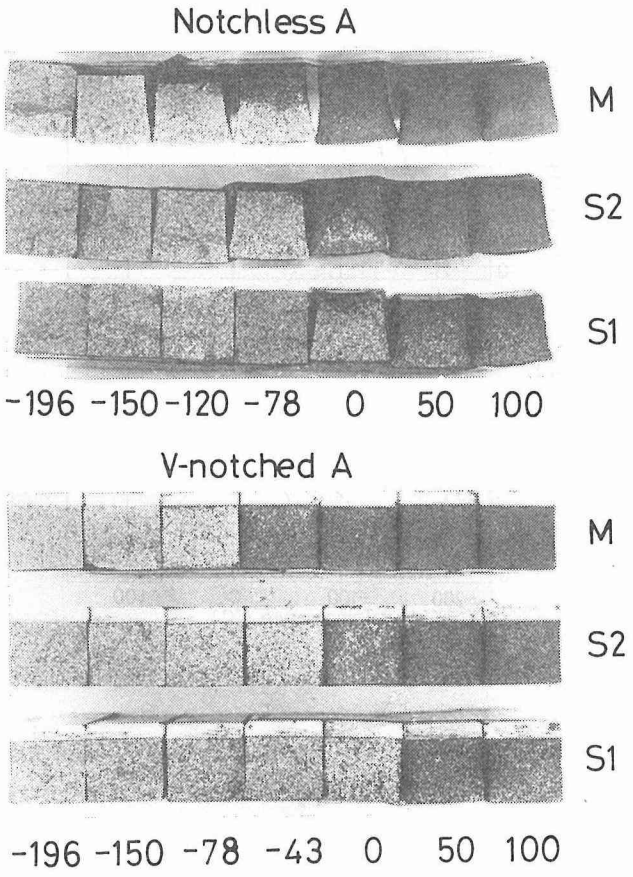

Fig. 5 Fracture appearance of A specimens

4. Macroscopic fracture appearance

Fig. 5 and 6 show the macroscopic fracture appearances of the specimens. The dark surface shows a ductile fibrous fracture and the bright surface is a brittle cleavage fracture. The fractures in every specimen changes from (1) all ductile to (2) partially brittle in the propagating region, then (3) ductile in the initiating region and brittle in the rest, and finally (4) all brittle. These fracture appearances correspond well with the energy transition curves. (1) and (2) correspond to the upper shelf of the curves, (4) is the lower shelf, and (3) is the transition range. In the notchless A specimens, the (2) to (3) transition occur at 0 to −78°C in S1A, at −78 to −120°C in S2A, and at −120 to −150°C in MA.

The relation of fracture appearance and the transition curve is similar in the V-notched specimens, and also in the notchless and V-notched B specimens. The energy transition temperatures in Table 3 conicide with the temperatures where the ductile fracture is restricted to a very limited initiation region and all of the remaining surface is brittle.

From the results, it is concluded that the transition occurs where a very small amount of ductile fracture causes general brittle fracture.

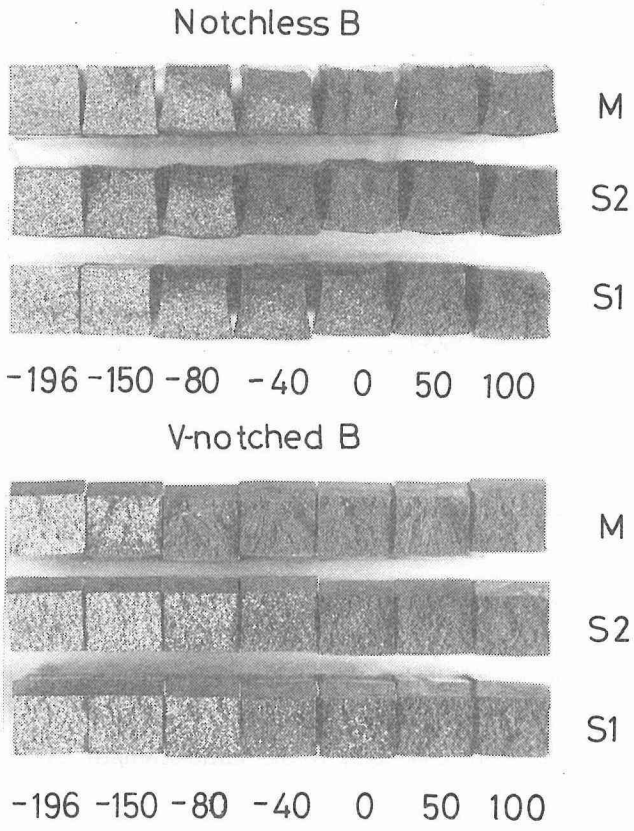

Fig. 6 Fracture appearance of B specimens

5. Load vs. time curves.

Load vs. time curves of notchless A specimens are shown in Fig. 7, and notchless B specimens in Fig. 8. The time axis in the figures can be regarded as the deflexion axis. Solid lines represent S1, long broken lines S2, and the short broken lines M.

In Fig. 7, the curves in the upper shelf region show that the specimen yields after elastic deformation, then shows work hardening, and ductile crack initiation around the maximum load, next stable crack propagation with decreasing load, and finally, unstable crack propagation with sudden decreases in the load. There are no significant differences in the deformation and fracture behaviors of S1A, S2A, and MA. Differences in impact energy are caused by differences in loads and deflextion at the final fracture.

In the low temperature region at the upper shelf, ductile cracks initiate around the maximum load and immediately propagate in an unstable manner without a stable propagation stage. At the lower shelf, cracks initiate at or even below the yield load, and propagate immediately, as a result there is no ductile region on the fractured surface. The energy and fracture appearance transition occurs where the crack initiates and propagates after the yielding but before sufficient plastic deformation.

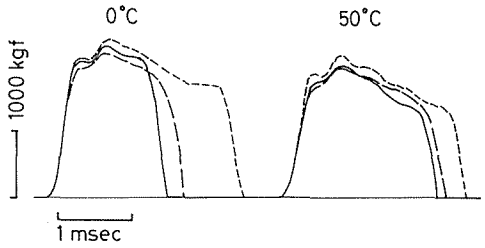

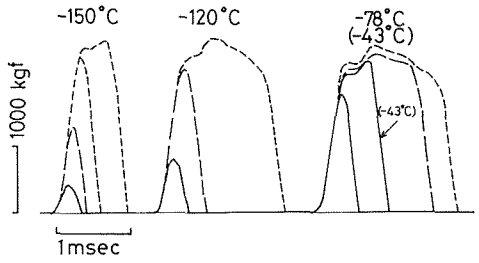

Fig. 7 Load vs. time curves, notchless A specimens

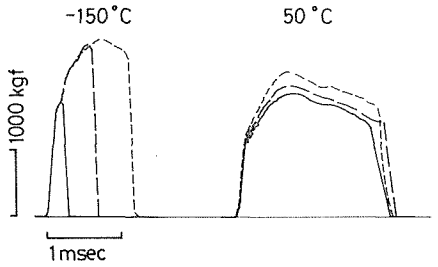

Fig. 8 Load vs. time curves, notchless B specimens

The B specimens behave similarly. At 50°C, all specimens are in the upper shelf, and there are no significant differences in the impact behavior of S1B, S2B, and SM, although there are differences in loads corresponding to the static strength. At −150°C, S1B is in the lower shelf showing crack initiation and propagation at yielding, S2B is in the transition range showing crack initiation and propagation between the yield and maximum loads, and MB is in the upper shelf exhibiting some stable ductile crack propagation.

With the B specimens, a higher resolution and quick response amplifier was used for the load time curve measurement. This revealed the differences in gradient of unstable crack propagation in upper shelf (50°C), smallest in S1B, intermediate in S2B, and largest in MB. This indicates that the energy absorption for unstable crack propagation with larger graphite nodules is larger in the ductile region. However, there is but little effect on the total impact energy because most of the Charpy energy is consumed in ductile crack initiation and stable propagation.

Load vs. time curves of V-notched B specimens are shown in Fig. 9. At 100°C, the maximum loads of S1B, S2B, and MB are similar but the deflexion is largest in S1B, medium in S2B, and smallest in MB. At 0°C, all specimens are in the upper shelf, the maximum load is the highest in MB and lowest in S1B, but the deflexion is largest in S1B and smallest in MB. The curves clearly show that the gradient of load decrease is smallest in S1B and largest in MB. This indicates that the crack propagation energy is the largest in S1B with the largest diameter graphite nodules, and the smallest in MB with the smallest nodules, likewise for the notchless B specimens. In V-notched specimens, however, the difference in propagation energy influences the total impact energy, and as the result, impact values are largest in S1B and smallest in MB.

Komatsu stated that[8], iron with smaller graphite nodules has lower resistance to ductile

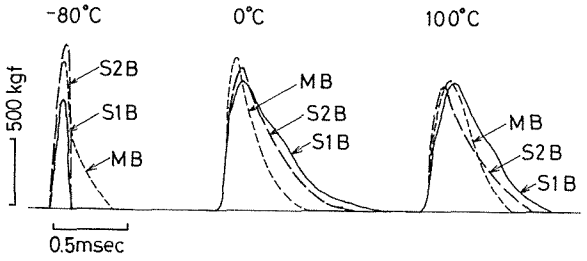

Fig. 9 Load vs. time curves, V-notched B specimens

crack propagation because large numbers of small nodules cause dimple nucleation and eases ductile crack propagation more than a small number of large nodules. The higher impact values of V-notched specimens with large graphite nodules in the present experiment can be explained by this mechanism.

At −80°C, S1B is in the brittle region showing crack initiation at low loads and immediate unstable rapid propagation ; S2B is brittle too, but the maximum load is higher than S1B, resulting in larger impact values than S1B ; MB is still in the ductile region, and the order of impact energy is in reverse of that at 0 and 100°C.

6. SEM fractography

Fig. 10 shows examples of SEM fractographs. Fig. 10-(1) is the fracture appearance near the tensile surface of S1A at −40°C, just at the transition. The surface consists mostly of dimples, large dimples with nuclei of graphite nodules and fine dimples in the ferrite matrix between graphite nodules. Cleavage fractures do not initiate directly from the graphite nodules, but at the fine dimple region away from the graphite nodules.

Fig. 10-(2) is the crack propagation region, and it shows almost all cleavage facets, and also some intergranular facets.

Fig. 10-(3) and (4) are the crack initiation and propagation region in sample MA at −150 °C at the transition. In the crack initiation region, large dimples are seen to be nucleated by graphite nodules, and cleavage cracks initiate from fine dimples between the graphite nodules. In the crack propagation region, the surface consists mostly of cleavages. Cleavage crack propagation appears to terminate at graphite nodules both in S1A and MA, and ferrite grain boundaries also appear to be barriers for the crack propagation.

Above the transition temperature, fracture surfaces consist mostly of dimples both near and away from tensile surface, with some cleavage facets in the propagation region, and more at lower temperatures. Below the transition temperature, fracture surfaces consist mostly of cleavages with a few dimples and intergranular facets such as in Fig. 10-(2) and (4). The results indicate that the specimens with smaller graphite nodules, and small ferrite grains, have larger resistance to brittle crack propagation, resulting in higher impact energies in the lower shelf region.

From the SEM fractography and the load time curves, the effect of graphite nodule size

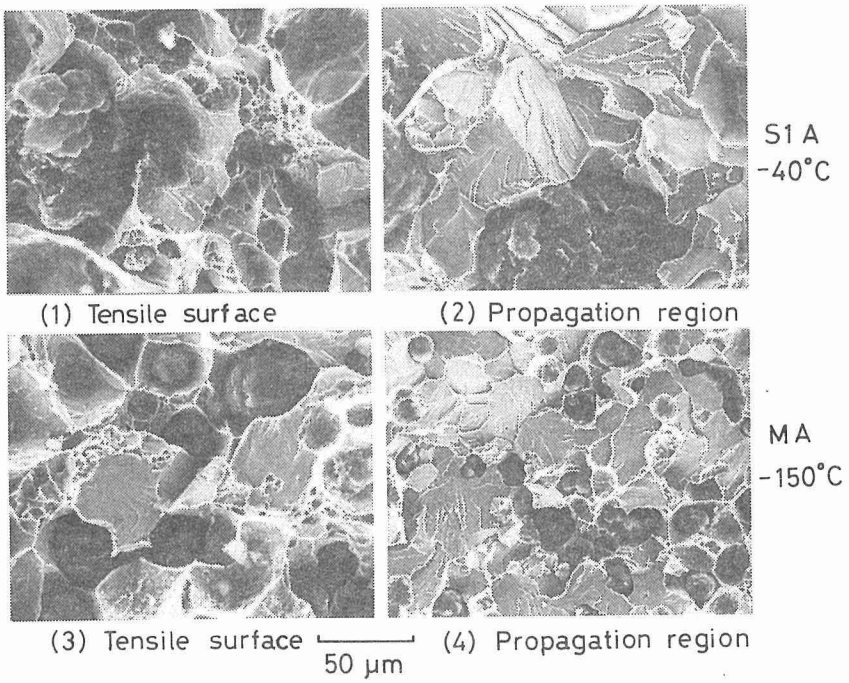

Fig. 10 SEM fractographs

may be concluded to be:

In the upper shelf, both crack initiation and propagation are by the dimple mechanism. There was no marked effect of graphite nodule size on the initiation and slow propagation of the ductile cracks, while large graphite nodules may contribute to the higher energy in unstable propagation.

In the transition range, crack initiation is ductile by the dimple mechanism, and cleavage cracks initiate from the ductile cracks away from graphite nodules. Large graphite nodules contribute to easier cleavage crack initiation by the larger inter-nodule distances. With increasing distance from the graphite nodules, the plane strain state, that is necessary for cleavage crack initiation becomes easier to achieve. With small graphite nodules however, the inter-nodule distance is short and the ductile crack front is more likely to be in the plane stress state. This agrees with Komatsu's conclusions on the influence of graphite nodule size on J_{IC} tests[8].

The graphite nodules act as barriers to cleavage crack propagation and the large number of small size nodules with small ferrite grains, result in a higher propagation energy.

7. Conclusions

Charpy impact tests were performed on ferritic spheroidal graphite cast irons with three different graphite nodule diameters, and the influence of nodule size on the transition behavior was discussed based on the fracture appearance, load time curves, and SEM

fractographs.

The results are:

1) The Charpy transition temperature of ferritic iron varied 50-100°C for 12-50 μm mean graphite nodule diameters while the static strengths were similar. The differences were large in high Si specimens and small in low Si specimens.

2) Impact load vs. time curves revealed that the resistance to unstable propagation of ductile cracks is large in specimens with larger graphite nodules. As a result, impact values in V-notched specimens are higher, while the effect was not apparent in notchless specimens.

3) The ductile to brittle transition occurs when cleavage cracks initiate from ductile cracks. The transition occurs earlier or with smaller deflexions with larger graphite nodules.

4) The energy transition terperature corresponds to the temperature where very small amounts of ductile cracks or dimples cause cleavage cracks to initiate, and the cracks to propagate in the brittle manner.

5) Large graphite nodules make it easier for cleavage cracks to initiate due to the large inter-nodule distances, which makes the plane strain state easy to achieve. In ferritic iron, cleavage cracks do not initiate directly from the graphite nodules in the transition range.

6) In the lower shelf, graphite nodules act as barriers to the crack propagation, and a large number of small graphite nodules contribute more to higher energy absorption than a small number of large graphite nodules.

7) There may be some effect of graphite nodules on twin generation, and intergranular fractures in the lower shelf region, but this is not predominant in the upper shelf and transition range.

Acknowledgment:

The authors wish to thank Mr. Hidetaka Torii (now in Mitsui Toatsu Chemicals) for his assistance with the experimental work.

References

(1) S. R. Holdsworth, G. Jolley, Int. Symp. Metall. Cast Iron, 2nd (1975), 809.
(2) R. Schofield, et al. Int. J. Pres. Ves. & Piping, 5 (1977), 73.
(3) A. Ikenaga, K. Okabayashi, IMONO (J. of JFS), 49 (1977), 411.
(4) T. Shioda, S. Komatsu, Zairyo (J. of JSMS), 30 (1981), 65.
(5) H. Sumimoto, K. Nakamura, IMONO, 55 (1983), 15.
(6) S. Nishi, T. Kobayashi, S. Taga, IMONO, 48 (1976), 10.
(7) B. Augland, British Welding J., 9 (1962).
(8) S. Komatsu, Doctoral Dissertation, Kinki Univ. (1989), 109.